Am J Transl Res 2021;13(9):10193-10205
www.ajtr.org /ISSN:1943-8141/AJTR0127837

Original Article

1-n-heptyl-5-(3, 4-difluorophenyl) biguanide inhibits non-small cell lung cancer cell growth by downregulating the EGFR signaling pathways

Di Xiao, Mei Peng, Yang Deng, Yayi Xiao, Xinyi Chen, Lan Ma, Bei Tang, Chenglin Guo, Xiaoping Yang

Key Laboratory of Study and Discovery of Small Targeted Molecules of Hunan Province, Key Laboratory of Protein Chemistry and Developmental Biology of Fish of Ministry of Education, Department of Pharmacy, School of Medicine, Hunan Normal University, Changsha 410013, Hunan, China

Received December 8, 2020; Accepted July 6, 2021; Epub September 15, 2021; Published September 30, 2021

Abstract: Lung cancer is among the diseases with the highest rates of morbidity and mortality. Our previous study found that a novel biguanide derivative, 1-n-heptyl-5-(3, 4-difluorophenyl) biguanide (8e) shows excellent anti-proliferative activity in non-small cell lung cancer (NSCLC) cell line A549. However, the underlying mechanism remains elusive. In this research, we analyzed the effect of 8e on NSCLC cell lines and explored the cell death mechanism caused by 8e. From our data, we found that 8e significantly decreased the cell activity and inhibited the colony formation of A549 and H1299 cells in a dose-dependent manner. Interestingly, this inhibitory effect of 8e was significantly reduced after silencing EGFR with lentiviral vectors. In contrast, after overexpressing EGFR in A549 and H1299, the lethality of 8e to the tumor cells increased. Simultaneously, we observed that 8e inhibited the expression of EGFR and its two essential downstream signaling pathways, AKT/mTOR and c-Raf/ERK1/2, and significantly reduced the activation of the EGFR pathway induced by EGF. Therefore, the results showed that 8e inhibits the proliferation of NSCLC cells by down-regulating the expression of EGFR, thereby inhibiting the downstream signaling pathway AKT/mTOR and c-Raf/ERK1/2. In addition, 8e also markedly reduces migration and induces the apoptosis of A549 and H1299 cells. *In vivo* results based on a lung cancer cell transplanted xenograft mouse model have further shown that 8e blocks A549 tumor growth without any significant hepatotoxicity or nephrotoxicity. These results indicate the high potential value of 8e as a candidate for treating NSCLC.

Keywords: Biguanide, cell proliferation, NSCLC, EGFR

Introduction

Lung cancer is the most common malignant tumor in the world, with the highest number of new cases and deaths [1]. According to clinical statistics, 80% of lung cancer patients are diagnosed with non-small cell lung cancer (NSCLC) [2]. In recent years, with great progress on the pathogenesis of NSCLC, great advances have been made in the treatment of NSCLC, but the five-year survival rate of NSCLC patients still does not exceed 20% [3, 4]. Thus, it's urgent to find novel drug candidates for treating NSCLC.

The epidermal growth factor receptor (EGFR), an important receptor, can mediate the response to the extracellular signals which promote the proliferation and migration of cancer cells [5]. According to previous studies, EGFR is abnormally high-expressed in various kinds of cancer tissues [6, 7]. After binding to ligands such as epidermal growth factor (EGF), EGFR and its downstream signaling pathway are activated and promote tumor genesis and development [8]. Similarly, EGFR is highly expressed in more than 60% of NSCLC patients [9]. Therefore, EGFR is considered a promising therapeutic target for NSCLC, and the FDA has approved EGFR inhibitors for cancer treatment, with EGFR as one of the most successful targets in treating cancer [10, 11]. Although NSCLC patients with abnormal EGFR upregulation usually respond significantly to gefitinib and erlotinib, two clinically approved anti-EGFR drugs, at the beginning of the treatment, almost all the patients will develop resistance and relapse

within one year [12]. Therefore, finding more effective anti-cancer drugs remains a difficult task. Zhu et al. reported that metformin can down-regulate the expression of EGFR in ErB2 breast cancer cells and inhibit their growth [13]. Our previous studies also demonstrated that metformin down-regulates the expression of EGFR and inhibits the proliferation and migration of muscle invasive bladder cell line T24 [14]. These results suggest that metformin may target EGFR to inhibit tumor proliferation. However, the effective concentrations of metformin to kill cancer cells are in the milli molar range, which makes metformin difficult for clinical application [15]. Moreover, we previously optimized the structure of biguanide and found that the compound 1-n-heptyl-5-(3, 4-difluorophenyl) biguanide (8e) (**Figure 1A**) has an excellent inhibitory effect on NSCLC cells [16]. However, the underlying mechanism remains elusive. In this study, we report on the mechanism of 8e against NSCLC.

Materials and methods

Cell culture

NSCLC cell lines (A549, H1299) were obtained from ATCC. All the cells were cultured in F12K (iCell) or RPMI-1640 (Hyclone) with 10% FBS (Hyclone) and 1% penicillin/streptomycin added and incubated at (37°C, 5% CO_2).

MTT assays

The effects of 8e on the viability of the NSCLC cell lines (A549, H1299) were determined using MTT assays. The cells were plated in 96-well plates (6.0×10^3/well) and incubated in a medium containing 10% FBS. After 12 h, the cells were treated with different concentrations of 8e for 72 h. Subsequently, the tetrazolium salt of MTT (50 μL; Sigma) was dissolved in Hank's balanced salt solution to a concentration of 2 mg/ml, and transferred to wells and incubated for 5 h. Lastly 150 μL of dimethyl sulfoxide (DMSO) was added to the plates to dissolve the formazan crystals, and the absorbance was gauged at 490 nm using a microplate reader (Biotek).

Clonogenic assays

The cells were plated in 24-well plates (8.0×10^3/well). After 24 h, the cells were treated with without 8e and left to grow for 6-8 days. Subsequently, the medium and drug in the 24-well plate were removed, and the remaining dead cells were washed with PBS. 10% formaldehyde solution was added to fix the cells for 1 h. Finally, 0.1% crystal violet was transferred to visualize the colonies for another 1 h. The absorbance was gauged at 550 nm with a microplate reader (Biotek).

Western blot

The protein extracts were loaded and run on SDS-PAGE which were then transferred to polyvinylidene fluoride (PVDF) membranes. The blots were blocked with 5% milk and then incubated with EGFR (CST), p-EGFR (1068, CST), p-AKT (CST), AKT (CST), p-mTOR (CST), mTOR (CST), p-c-Raf (CST), p-ERK1/2 (CST), ERK1/2 (CST), and β-actin (CST) overnight at 4°C. After they were washed for 30 minutes using TBST, the blots were incubated with the secondary antibodies. After they were washed with PBS again, the blots were visualized using a Chemi-Doc system (Tanon 4600, Shanghai, China).

Measurement of the cell migration

4×10^4 serum starved cells were plated in the upper chamber of a transwell system in the absence or presence of 8e. A medium containing 10% FBS was added to the lower chambers. After 24 hours, 4% formaldehyde solution was used to fix the cells, and subsequently, 0.1% crystal violet was transferred to visualize the stained cells. The membranes were cleaned, air-dried, and photographed with a DFC450C microscope (Leica).

Apoptosis

The cell apoptosis was gauged using flow cytometry after the 8e treatment. In brief, the A549 and H1299 cells were plated in 6-well plates and treated with or without 8e for 24 h. Then the cells were harvested using trypsinization and washed twice with PBS. Subsequently, the cells were resuspended in 200 μL of 1× binding buffer and stained in the dark at RT (25°C) with 5 μl of FITC Annexin V. Finally, the cells were diluted with 400 μL of 1× binding buffer and measured using a FACS Calibur flow cytometer (Becton, Dickinson and Company, USA).

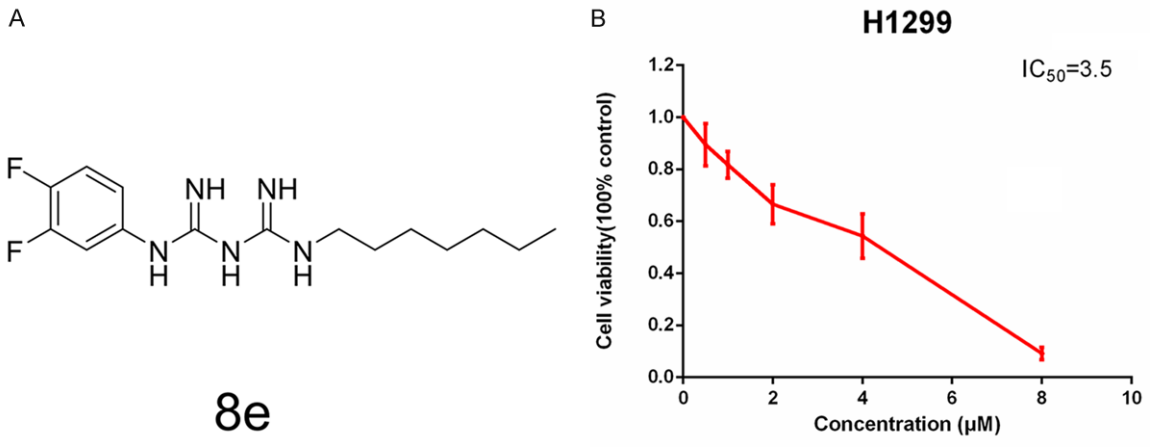

Figure 1. The effect of 8e on the proliferation of H1299. A. The chemical structure of 8e. B. H1299 was treated with different concentrations of 8e for 72 h. Later, an MTT solution was transferred to the wells and incubated for 5 hours, then finally, DMSO was added to the plates and the absorbance was gauged at 490 nm using a microplate reader. The IC_{50} of 8e in H1299 was calculated using SPSS 20.0. ($^{*}P<0.05$, $^{**}P<0.01$, $^{***}P<0.001$, n=3).

The knockdown or overexpression of EGFR using transfection lentiviral vectors

The EGFR knockdown lentiviral vectors shCtrl, shEGFR-1, shEGFR-2, shEGFR-3 (Table S1), the EGFR overexpression lentiviral vectors, the overexpression Ctrl (OC), and the overexpression EGFR (OE) were purchased from GeneChem Co. Ltd. (China). Briefly, the lentiviruses and 40 μl transfection reagents (GeneChem, China) were transferred to 1 mL of complete culture medium to replace the original culture medium. After 12 hours, the cells were cultured with a normal complete medium again. Three days later, puromycin was added to the cell culture flask to kill the untransfected cells.

Subcutaneous xenograft model study

Female BALB/c nude mice (n=18) were purchased from the Hunan SJA Laboratory Animal Co., Ltd (China). The study protocol was approved by the Ethics Committee of Hunan Normal University (Protocol 2020005). A 10^7 A549 cell suspension was injected subcutaneously into the mice to establish a xenograft tumor model. When the tumors grew to 80-100 cm^3, the mice were randomly divided into three groups: Group I (n=6) — the control group without treatment. Group II (n=6) — the tumor group with vehicle treatment. Group III (n=6) — the tumor group with 8e treatment. The 8e was diluted with 2%DMSO+5%PEG-400+5%Tween-80+88%water and administered at 8 mg/kg/d, via i.p. injections. The tumor volumes and the mice's weights were gauged every two days. The tumor volumes were calculated according to the formula: 1/2× long diameter × short diameter^2. On the final day of the experimental procedure, the mice were sacrificed and their livers and kidneys were removed, paraffin-embedded, sectioned, and analyzed using HE.

Statistical analysis

The data from the three independent experiments were expressed as the mean ± SD. The statistical analysis was performed with SPSS 20.0. The statistical analysis was performed using Student's t-tests. $P<0.05$ was considered statistically significant.

Results

The anti-cancer proliferative effect of 8e on the H1299 cells

Our previous study determined that 8e has a strong inhibitory effect on NSCLC cell line A549 [16]. Therefore, we further tested the anti-proliferative activity of 8e against NSCLC cell line H1299 using MTT assays. The results showed that 8e inhibited the H1299 cell proliferation in a dose-dependent manner (**Figure 1B**).

The EGFR expression was closely related to the cell proliferation

Studies have proved that EGFR is closely related to the proliferation of NSCLC [17]. In this

study, to further examine the function of EGFR in NSCLC development, we established three stable EGFR-knockdown clones and one stable over-expressed EGFR clone in two cell lines. After killing the untransfected cells with puromycin to bring the successful transfection ratio to 100% (Figure S1), the EGFR levels in the stably regulated lung cancer cells after knockdown or overexpression were verified through a Western blot analysis, and we found that shEGFR-2 has the best silencing effect (**Figures 2A**, **2B** and **3F**), so we chose shEGFR-2 lentiviral vectors and OE lentiviral vectors for further experiments. Our study also found that the knockdown of EGFR expression dramatically reduced the rate of cell growth compared with the shCtrl group using MTT (**Figure 2C**, **2E**). In addition, the knockdown of EGFR inhibited the rate of colony formation (**Figure 2D**, **2F**). These data suggest that the EGFR expression is closely related to the proliferative abilities of the A549 and H1299 cells. Therefore, any strategy for downregulating the expression of EGFR may be a feasible way of treating patients with high EGFR expressions.

8e inhibits NSCLC cell proliferation and colony formation via inhibiting EGFR

To further investigate whether the 8e inhibition of cell proliferation is related to EGFR, we measured the EGFR levels after six hours of 8e treatment. As we can see in **Figure 3A**, the EGFR and phosphorylated EGFR levels were significantly reduced in the A549 and H1299 cells after the 8e treatment, indicating that 8e inhibited the proliferation of the NSCLC cells by targeting EGFR. To further verify this finding, we confirmed that knocking down the expression of EGFR reduced the inhibition of 8e on the proliferation and colony formation of the A549 and H1299 cells (**Figure 3B-E**). In contrast, the EGFR overexpression effectively enhanced the inhibition of cell proliferation induced by the 8e treatment. As shown in **Figure 3G**, **3I**, the antiproliferative activity of 8e with an IC_{50} value of 4.6 μM for OC-A549, 3.1 μM for OC-H1299 was higher than the IC_{50} value of 2.5 μM for OE-A549, 1.9 μM for OE-H1299. Similarly, the A549 and H1299 cells with stable EGFR overexpressions were characterized by a higher 8e induced inhibition of colony formation (**Figure 3H**, **3J**). These results forcefully demonstrated that 8e inhibits cell proliferation and colony formation by regulating the EGFR levels.

8e inhibits the EGFR signaling pathway

Our results above showed that 8e can inhibit the expression of EGFR (**Figure 3A**), and then we discussed the specific mechanism of 8e for regulating cell proliferation. Previous studies showed that AKT/mTOR and c-Raf/ERK1/2 are two important downstream signaling pathways of EGFR, the overexpression of which was strongly associated with the development of tumors [18]. Therefore, we further studied the protein level changes of AKT/mTOR and c-Raf/ERK1/2 after the 8e treatment. The Western blot results showed that 8e significantly blocked the AKT/mTOR and c-Raf/ERK1/2 phosphorylation levels at the concentrations of 2 μM and 4 μM without changing their total protein levels (**Figure 4A**, **4B**).

8e blocked the ligand-induced activation of the EGFR signaling pathway

As we know, EGFR is activated when it is stimulated by EGF. Therefore, we further investigated whether 8e could inhibit the activation of EGFR and its downstream signaling pathways in the presence of EGF. Our data indicated that the stimulation of EGF dramatically up-regulated the phosphorylation of EGFR, while the 8e treatment significantly reduced the EGF-induced p-EGFR protein level (**Figure 5A**, **5B**). Simultaneously, the EGF stimulation up-regulated p-AKT/p-mTOR and p-c-Raf/p-ERK1/2, However, this effect was significantly weakened by the 8e treatment (**Figure 5A**, **5B**). Therefore, our results suggest that 8e inhibits NSCLC cell proliferation by inhibiting EGFR and its two important downstream signaling pathways, including AKT/mTOR and c-Raf/ERK1/2, and blocks the ligand-induced activation of the EGFR signaling pathway.

8e inhibited NSCLC cell migration and induced apoptosis

To investigate the effect of 8e on cell migration and apoptosis, two NSCLC cell lines were treated with different concentrations of 8e, and the cell migration and apoptosis levels were monitored. As shown in **Figure 6A**, **6B**, the cell migration was overtly inhibited after the 8e treatment, and the degree of migration inhibi-

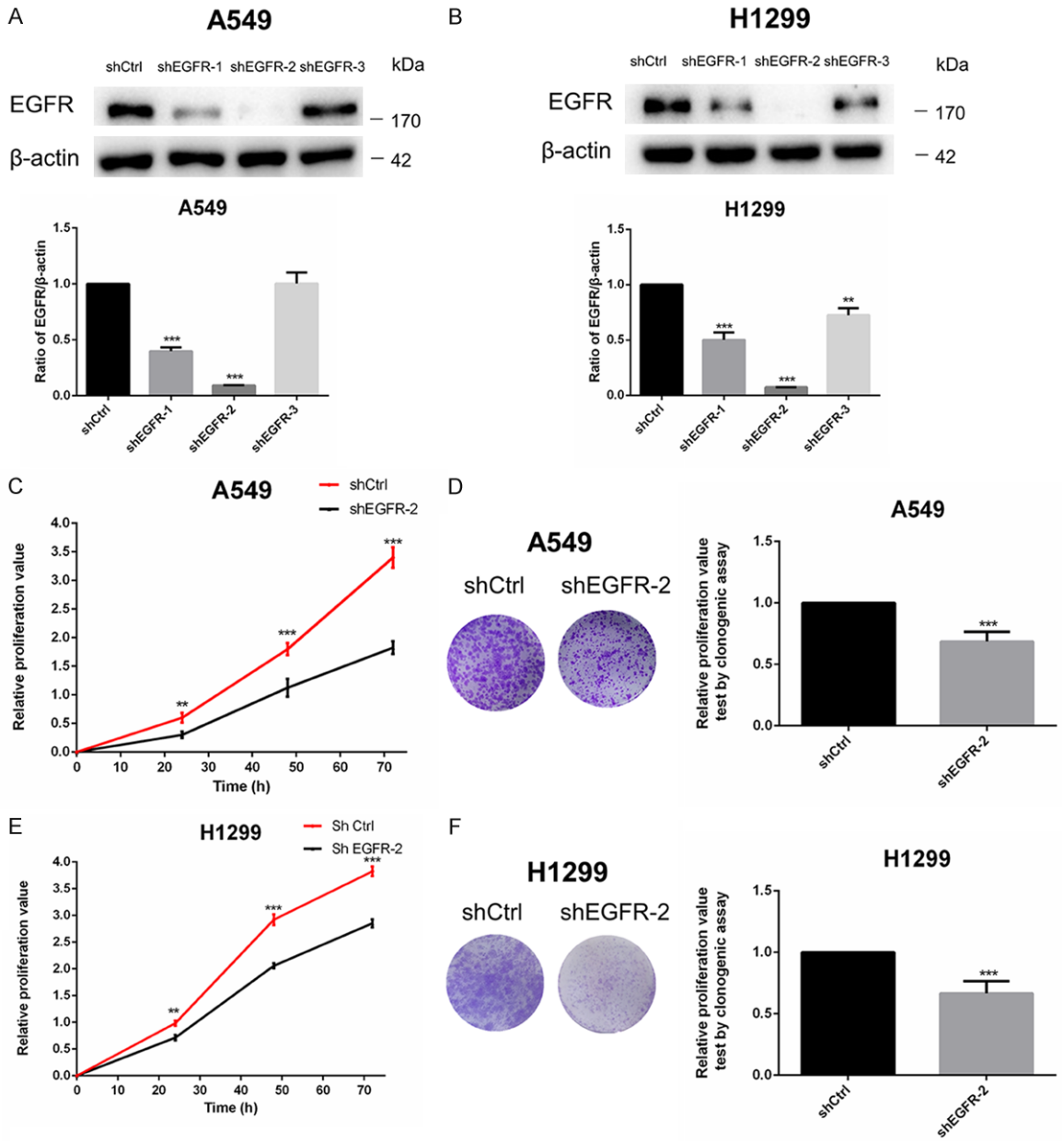

Figure 2. The effect of EGFR expression on the cell proliferation. A, B. The EGFR expression was determined using WB after the stable transfection with three EGFR lentiviral silencing vectors in A549 and H1299. C. The A549 cells were plated in 96-well plates, and MTT was added at 24, 48, and 72 h after the cell morphologies were formed to measure the absorbance. D. The A549-shCtrl and A549-shEGFR-2 cells were seeded on a 24-well plate. After 7 days, the cells were fixed with 4% formalin for 2 hours and then stained with 0.1% crystal violet for 2 hours. The absorbance was gauged at 550 nm using a microplate reader. E. The H1299 cells were plated in 96-well plates, and MTT was added at 24, 48, and 72 h after the cell morphologies were formed to measure the absorbance. F. H1299-shCtrl and H1299-shEGFR-2 cells were seeded on a 24-well plate. After 7 days, the cells were fixed with 4% formalin for 2 hours and then stained with 0.1% crystal violet for 2 hours. The absorbance was gauged at 550 nm using a microplate reader. (*P<0.05, **P<0.01, ***P<0.001, n=3).

tion was increased with the increasing concentrations of 8e. We used Annexin-V apoptosis kits to determine the apoptosis levels. As shown in **Figure 6C**, **6D**, compared with the untreated group, the apoptosis in the 8e treatment group significantly increased in a dose-dependent manner. These results indicate that 8e can not only inhibit cell proliferation, but it

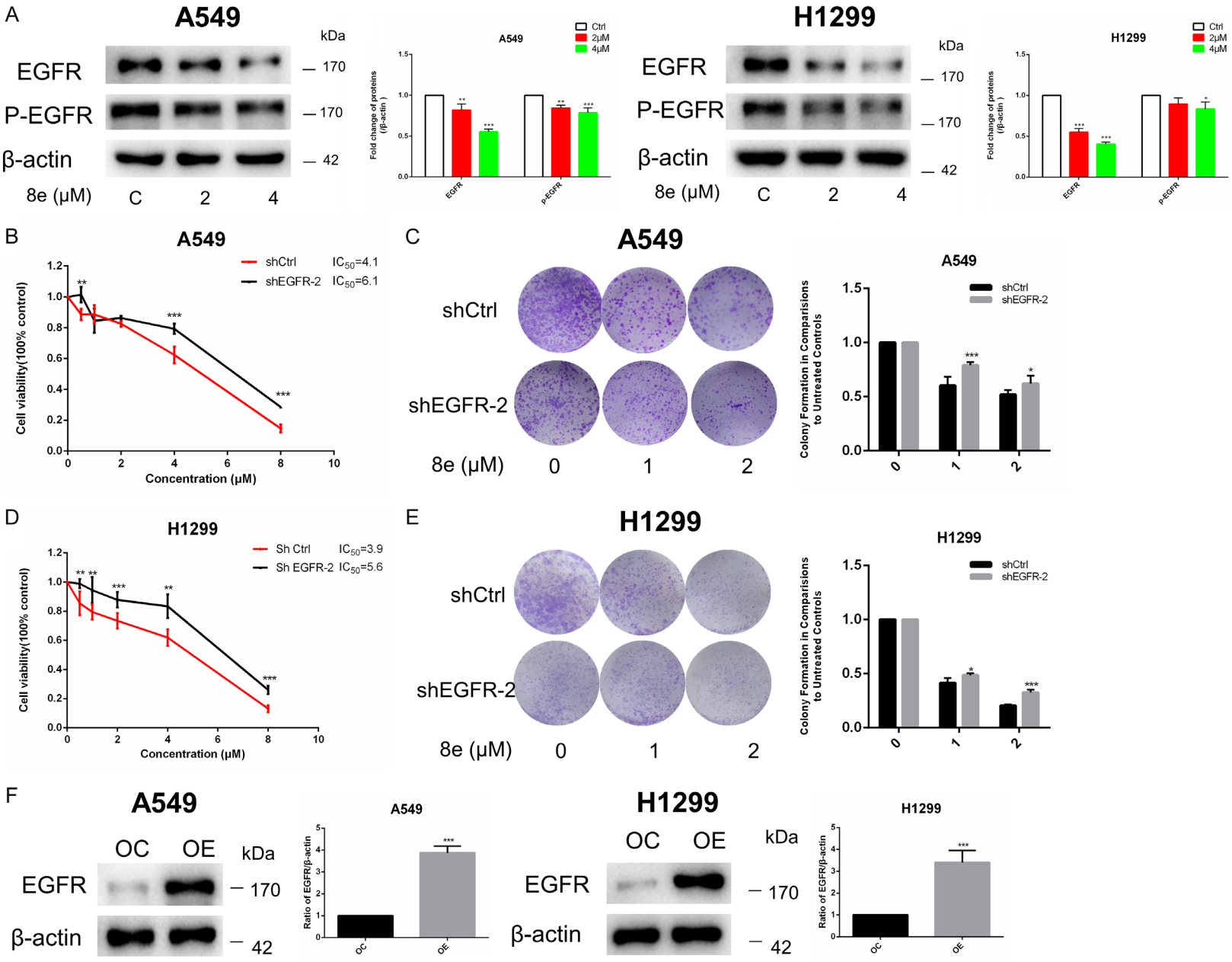
A
A549
kDa
EGFR
P-EGFR
β-actin
170
170
42
8e (μM) C 2 4
A549
Ctrl
2μM
4μM
Fold change of proteins (β-actin)
EGFR
p-EGFR
H1299
B
A549
shCtrl IC50=4.1
shEGFR-2 IC50=6.1
Cell viability(100% control)
Concentration (μM)
C
A549
shCtrl
shEGFR-2
8e (μM) 0 1 2
Colony Formation in Comparisions to Untreated Controls
D
H1299
Sh Ctrl IC50=3.9
Sh EGFR-2 IC50=5.6
E
H1299
F
A549
OC OE
Ratio of EGFR/β-actin
H1299

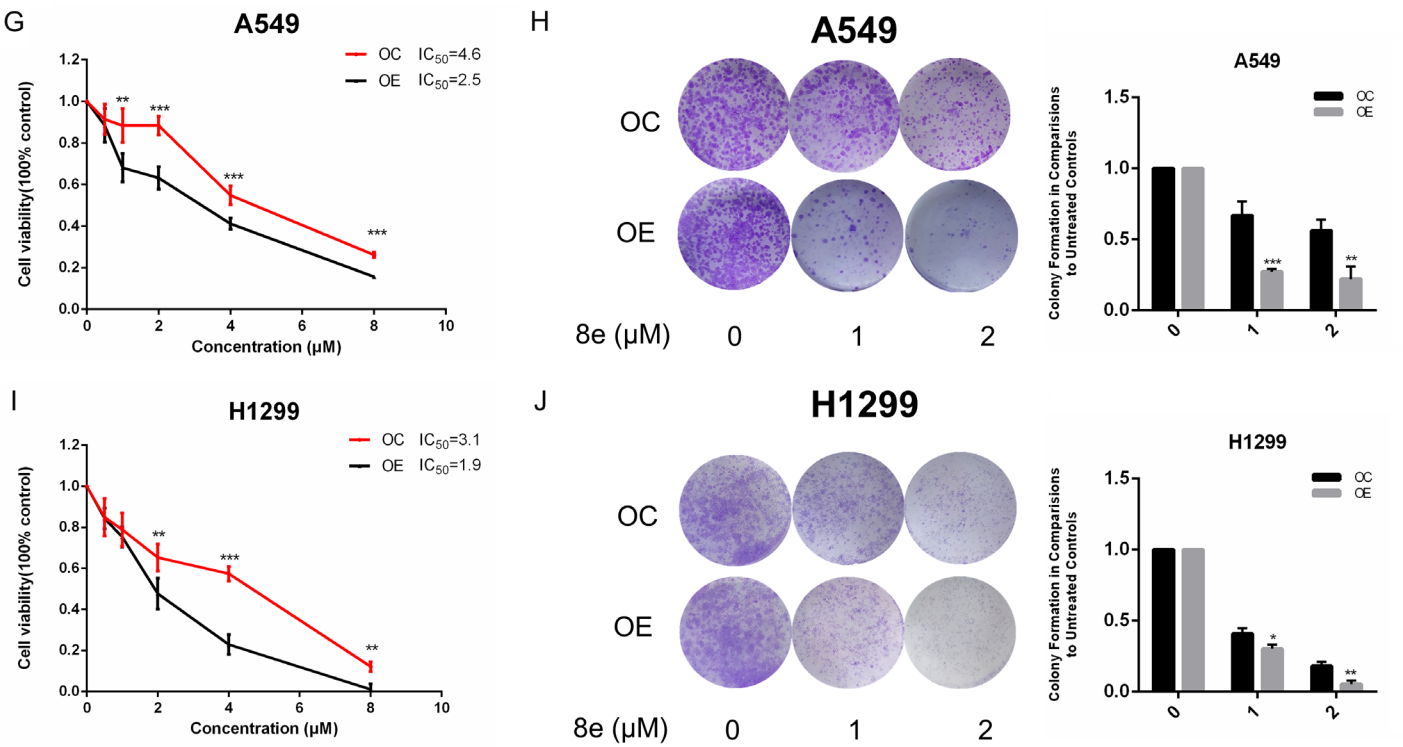

Figure 3. 8e reduced the A549 proliferation mediated by EGFR. (A) A549 and H1299 were starved for 12 h and then treated with 8e for 6 h, and the levels of the total or phosphorylated EGFR were determined using WB. (B, D) A549-shCtrl (B), A549-shEGFR-2 (B) and H1299-shCtrl (D), H1299-shEGFR-2 (D) cells were treated with different concentrations of 8e for 72 h. Later, MTT solution was transferred to the wells and incubated for 5 hours, and finally, DMSO was added to the plates and the absorbance was gauged at 490 nm using a microplate reader. (C, E) A549-shCtrl (C), A549-shEGFR-2 (C) and H1299-shCtrl (E), H1299-shEGFR-2 (E) cells were seeded on a 24-well plate and treated with different concentrations of 8e for 7 days, then the cells were fixed with 4% formalin for 2 hours and then stained with 0.1% crystal violet for 2 hours. The absorbance was gauged at 550 nm using a microplate reader. (F) The EGFR expression was measured using WB after the stable transfection with the EGFR lentiviral overexpression vectors in A549 and H1299. (G, I) A549-OC (G), A549-OE (G) and H1299-OC (I), H1299-OE (I) cells were treated with different concentrations of 8e for 72 h. Later, the MTT solution was transferred to the wells and incubated for 5 hours, and finally, DMSO was added to the plates and the absorbance was gauged at 490 nm using a microplate reader. (H, J) A549-OC (H), A549-OE (H) and H1299-OC (J), H1299-OE (J) cells were seeded on a 24-well plate and treated with different concentrations of 8e for 7 days, and then the cells were fixed with 4% formalin for 2 hours and then stained with 0.1% crystal violet for 2 hours. The absorbance was gauged at 550 nm using a microplate reader. (*P<0.05, **P<0.01, ***P<0.001, n=3).

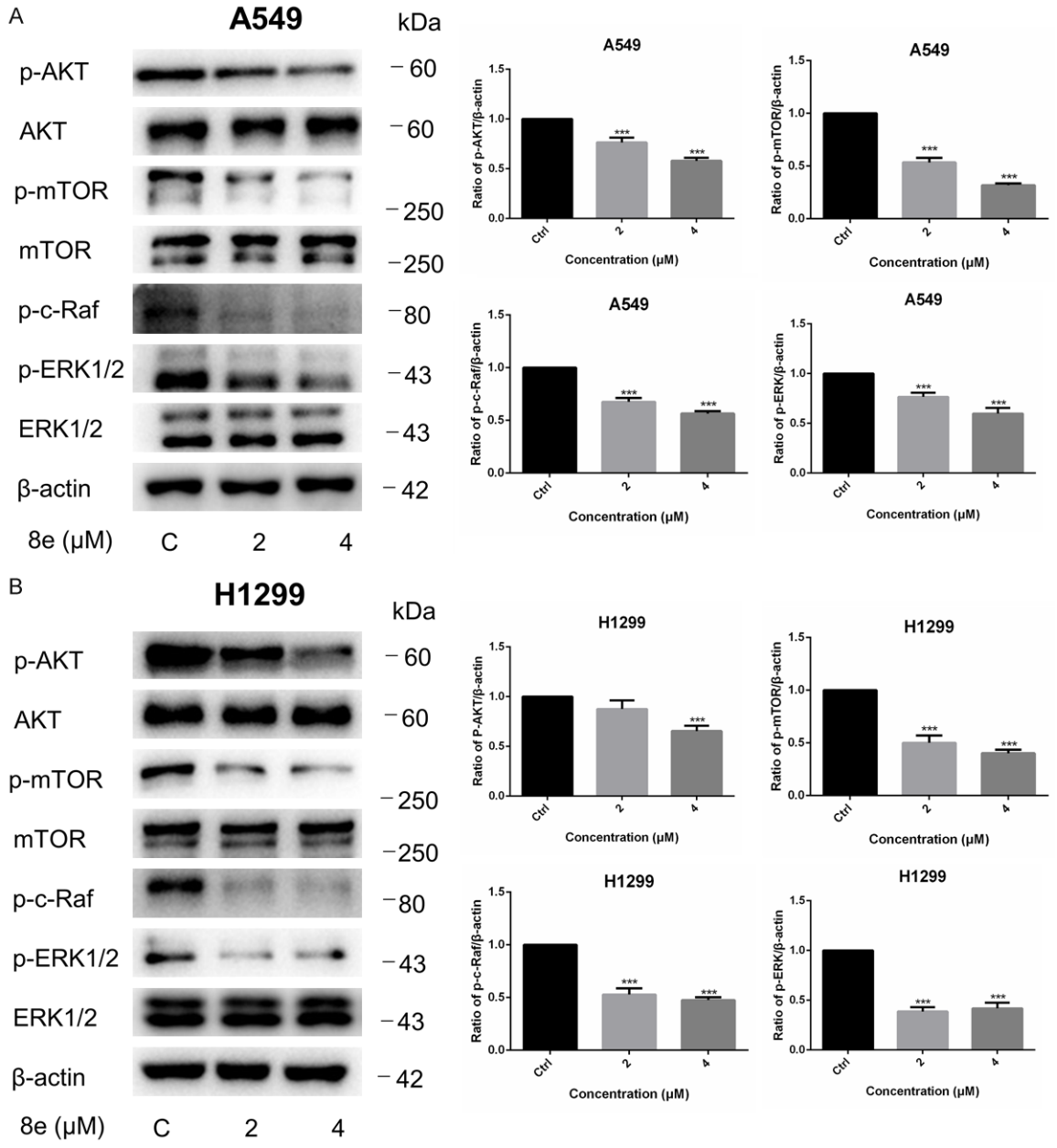

Figure 4. The effect of 8e on the expression of EGFR-AKT/mTOR and c-Raf/ERK1/2. A, B. Two NSCLC cell lines were starved for 12 h and then treated with an increasing concentration of 8e for 6 h, and the levels of total or phosphorylated AKT/mTOR and c-Raf/ERK1/2 were measured using WB (*P<0.05, **P<0.01, ***P<0.001, n=3).

can also significantly reduce cell migration and induce cell apoptosis.

The in vivo efficacy of 8e on the growth of the A549 cell transplanted xenografts

Since 8e has a strong inhibitory effect on lung cancer cells, we continued to evaluate the antitumor activity of 8e *in vivo*. 13 days after the tumor transplantation, the mice were grouped and treated with 8e. As show in **Figure 7A**, **7B**, the growth of the subcutaneously transplanted tumors was distinctly suppressed in the 8e treatment group. After 28 days, the solid tumors were harvested and weighed. Compared with the control group, the tumor weights of the 8e treatment group were reduced by 71% (**Figure 7C**). Importantly, the average weight of the mice in the 8e treatment group did not drop during the treatment period (**Fi-**

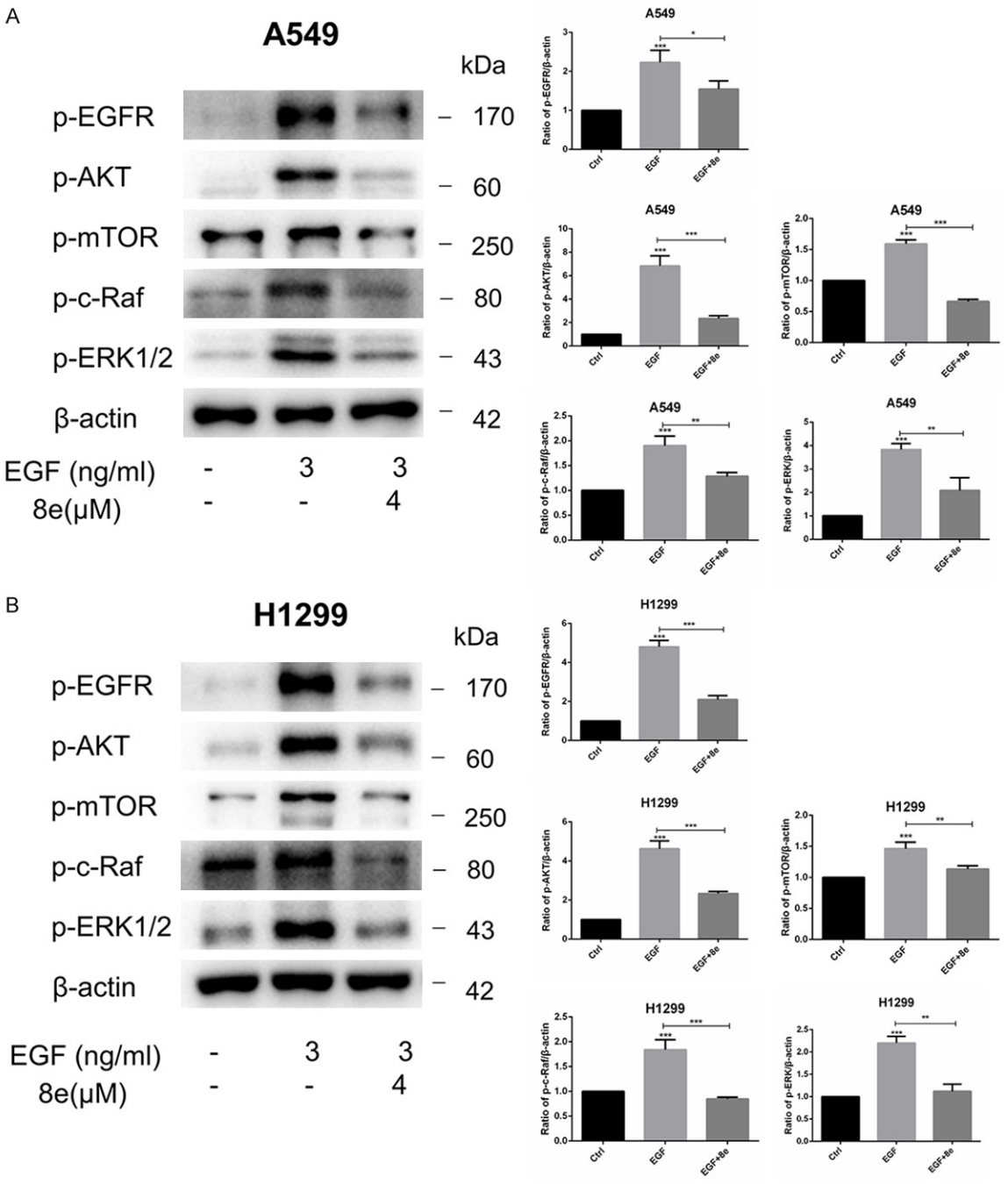

Figure 5. The effect of 8e on the EGF induced activation of EGFR. (A, B) The A549 and H1299 cells were starved for 12 h, then pretreated with 8e for 6 h and later treated with EGF for 30 min. The phosphorylated EGFR, AKT/mTOR, and c-Raf/ERK1/2 levels were measured using WB. Our statistical analysis determined the ratios of the optical density values of these proteins to β-actin (*P<0.05, **P<0.01, ***P<0.001, n=3).

gure 7D). Our preliminary results showed that the cytotoxicity of 8e to human umbilical vein endothelial cells was much less than the cytotoxicity of cancer cell line A549. Thus, we further monitored whether the use of 8e could cause any toxicity *in vivo* by determining the morphological alterations of liver and lung tissues in this animal experiment. The data showed that 8e didn't exhibit any toxicity in these liver and kidney tissues collected from the treatment group compared with the control group (**Figure 7E**). These data suggest that 8e

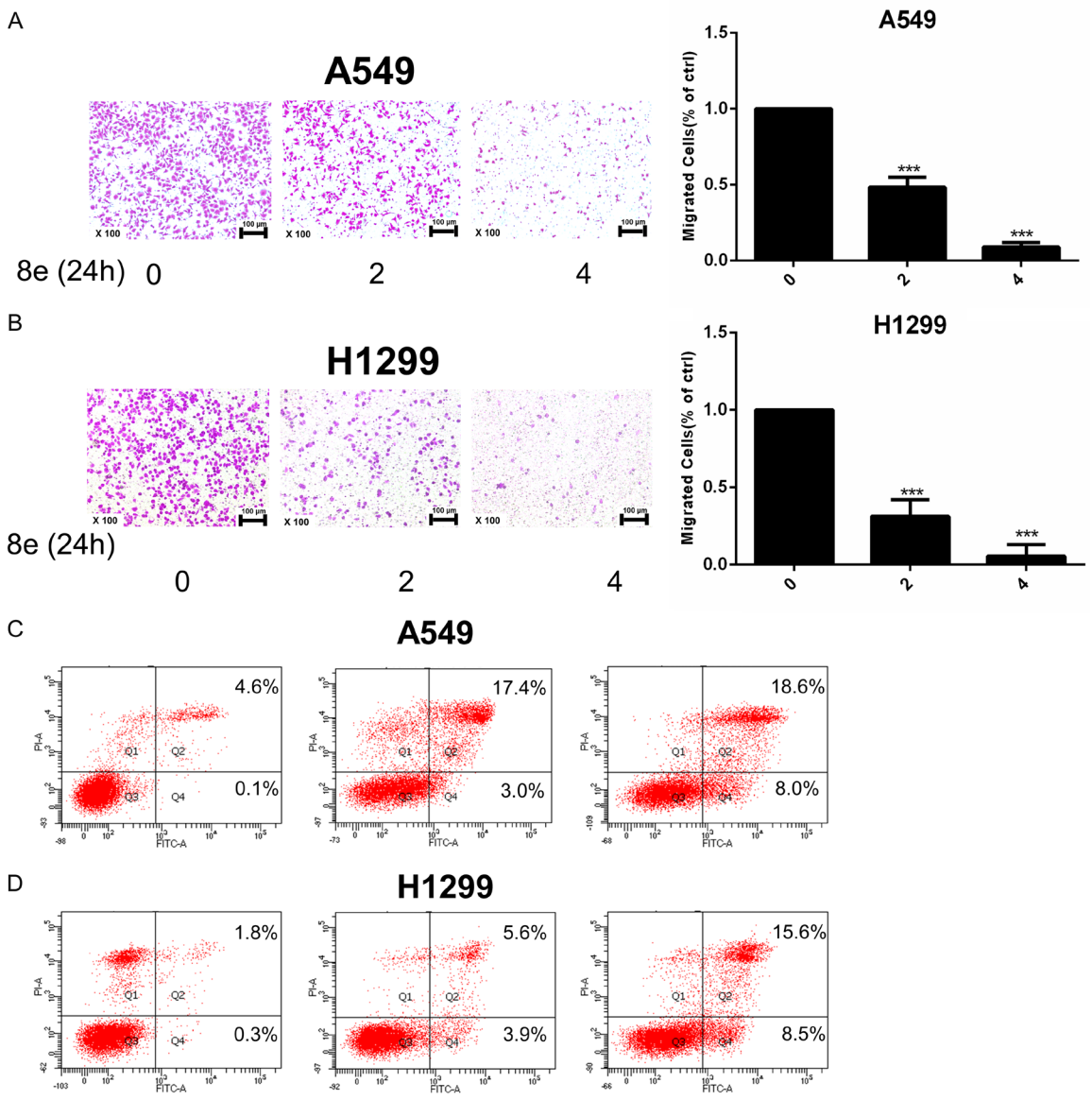

Figure 6. The effect of 8e on the cell migration inhibition and induction of apoptosis. A, B. The cells were plated in the upper chamber of a Transwell plate and then treated with 8e. After 24 hours, the chamber was taken out and the cells were fixed with 4% formalin and then stained with 0.5% crystal violet. Finally, the cells in the upper part of the chamber were wiped off and photographed with a microscope. C, D. The effect of 8e on apoptosis. The A549 and H1299 cells were treated with 8e at concentrations of 8 μM and 10 μM for 24 h. Representative flow cytometry scatter plots showing propidium iodide (y axis) and annexin V FITC (x axis) staining. Quantitation of the flow cytometry experiments ($^{*}P<0.05$, $^{**}P<0.01$, $^{***}P<0.001$, n=3).

may be a potent anti-NSCLC drug without any significant hepatotoxicity or nephrotoxicity.

Discussion

EGFR, a transmembrane receptor, consists of an extracellular ligand binding domain, a transmembrane domain, and an intracellular domain [19]. The unique structure of EGFR allows the signal to travel from the outside of the cell membrane to the inside of the cell to regulate the cell growth. When a ligand binds to EGFR, it causes EGFR dimerization and phosphorylation to activate the downstream signaling pathways, including the RAS/RAF/ERK1/2/MAPK pathway and the PI3K/AKT/mTOR pathway [8]. The abnormal high expression of these pathways is closely related to the growth and proliferation of the cancer cells [20]. Wu et al. showed that traditional Chinese medicine

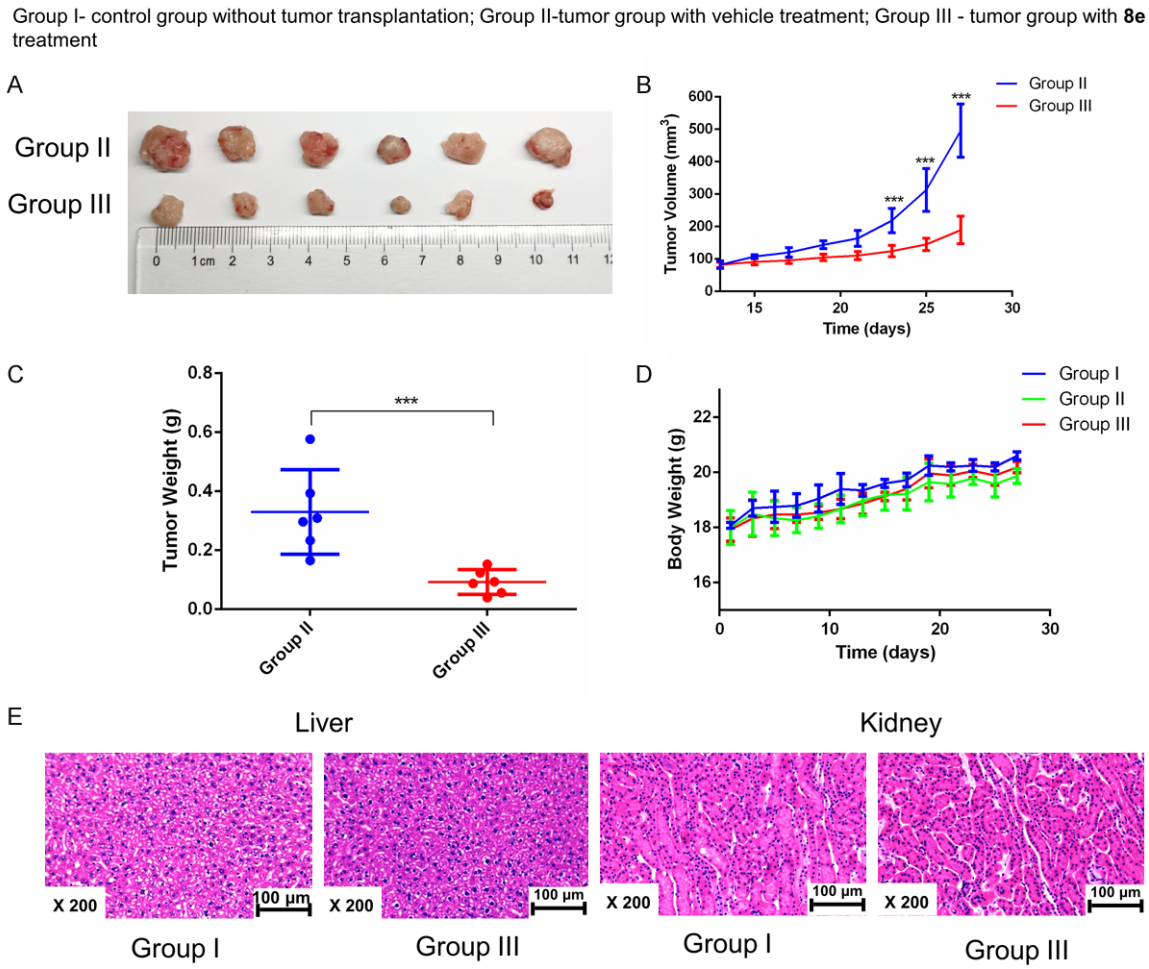

Figure 7. The *in vivo* effect of 8e on the growth of the A549 cell transplanted xenografts. A. The 10^7 A549 cell suspension was injected subcutaneously into the mice, then after 13 days, the mice with tumors were equally divided into two groups, and the mice in Group II were treated with the vehicle, and the mice in Group III were treated with 8e. After 28 days, the solid tumors were taken out and photographed with a phone. B. After the mice were treated with 8e, the tumor volume of each mouse was measured every two days and the average tumor volume in each group was calculated to create the figure. C. The solid tumors were taken out and weighed, and the average weights of each group's tumors were calculated to create the figure. D. After the mice were injected with the tumor cells, the mice's weights were measured every two days. And the average weight of the mice in each group was calculated to create the figure. E. The livers and kidneys of the mice in Group I and Group III were taken out and observed using HE staining to see if the mice had hepatotoxicity or nephrotoxicity after the 8e treatment. ($^*P<0.05$, $^{**}P<0.01$, $^{***}P<0.001$, n=6).

CFF-1 inhibits EGFR autophosphorylation and reduces EGFR activity, thereby blocking the activation of the PI3K/AKT and c-Raf/ERK1/2 pathways to induce the inhibition of prostate cancer cell growth, autophagy, and apoptosis [21]. Li's study indicates that Herbacetin controls malignant melanoma processes by inhibiting both EGF-induced phosphorylation or autophosphorylation and accelerating the degradation of EGFR, thereby further inhibiting AKT and ERK1/2 phosphorylation [22]. Our previous study found that 8e has great anti-proliferation and anti-clonal colony formation effects on NSCLC A549 cells, and the effect of 8e on inhibiting NSCLC cells is closely related to the EGFR expression, which led us to further explore the downstream effect of the EGFR pathway on 8e's anti-proliferation. Since AKT/mTOR and c-Raf/ERK1/2 are two essential downstream signaling molecules which play a key role in tumorigenesis, tumor progression and metastasis in various types of tissue cells [8], we further measured the p-mTOR, p-AKT, p-c-Raf and p-ERK1/2 levels using Western

blot. As expected, 8e significantly inhibited their phosphorylation and blocked the function of EGF. Therefore, for the first time we determined that compound 8e not only induces NSCLC cell growth inhibition via targeting the EGFR signaling pathways and blocks the EGF-induced activity of the AKT/mTOR and c-Raf/ERK1/2 signal pathways, but it also inhibits cell invasion and induces apoptosis. The animal results in the present study show that 8e treatment can markedly reduce tumor volume and tumor weight without any hepatotoxicity or nephrotoxicity. In conclusion, our study may partly provide a molecular basis for the future clinical treatment of NSCLC with 8e.

Acknowledgements

This work was supported by the National Natural Science Foundation of China (No. 81874212), the Creative Project for College Students (No. S202010542009), the Huxiang High-Level Talent Innovation Team (2018RS3072), the Opening Fund for Key Laboratory of Molecular Pharmacology and Drug Evaluation (Yantai University), Ministry of Education (P201905), the Scientific and Technological Projects for Collaborative Prevention and Control of Birth Defects in Hunan Province (2019SK1012), and the Key Grant of Research and Development in Hunan Province (2020DK2002).

Disclosure of conflict of interest

None.

Abbreviations

NSCLC, Non-small cell lung cancer; EGFR, Epidermal growth factor receptor; EGF, Epidermal growth factor; DMSO, Dimethyl sulfoxide; OC, Overexpression control; OE, Overexpression EGFR; SDS-PAGE, Sodium dodecyl sulphate polyacrylamide gel electrophoresis; PVDF, Polyvinylidene fluoride; TBST, Tris-buffered saline with 0.1% Tween.

Address correspondence to: Xiaoping Yang, Key Laboratory of Study and Discovery of Small Targeted Molecules of Hunan Province, Department of Pharmacy, School of Medicine, Hunan Normal University, Changsha 410013, Hunan, China. Tel: +86-15874066132; Fax: +86-15874066132; E-mail: xiaoping.yang@hunnu.edu.cn

References

[1] Bray F, Ferlay J, Soerjomataram I, Siegel RL, Torre LA and Jemal A. Global cancer statistics 2018: GLOBOCAN estimates of incidence and mortality worldwide for 36 cancers in 185 countries. CA Cancer J Clin 2018; 68: 394-424.

[2] Li P, Lv X, Zhang Z and Xie S. S100A6/miR193a regulates the proliferation, invasion, migration and angiogenesis of lung cancer cells through the P53 acetylation. Am J Transl Res 2019; 11: 4634-4649.

[3] Molinier O, Goupil F, Debieuvre D, Auliac JB, Jeandeau S, Lacroix S, Martin F and Grivaux M. Five-year survival and prognostic factors according to histology in 6101 non-small-cell lung cancer patients. Respir Med Res 2020; 77: 46-54.

[4] Yang L, Wen Y, Lv G, Lin Y, Tang J, Lu J, Zhang M, Liu W and Sun X. α-Lipoic acid inhibits human lung cancer cell proliferation through Grb2-mediated EGFR downregulation. Biochem Biophys Res Commun 2017; 494: 325-331.

[5] Xu L, Wu H, Jiang C, Wang H, Gao B, Yan S, Qi Y and Zhou S. Dacomitinib, a new pan-EGFR inhibitor, is effective in killing ovarian cancer cells. Discov Med 2016; 22: 297-309.

[6] Li F, Liu Y, Chen H, Liao D, Shen Y, Xu F and Wang J. EGFR and COX-2 protein expression in non-small cell lung cancer and the correlation with clinical features. J Exp Clin Cancer Res 2011; 30: 27.

[7] Wang L, Yao J, Shi X, Hu L, Li Z, Song T and Huang C. MicroRNA-302b suppresses cell proliferation by targeting EGFR in human hepatocellular carcinoma SMMC-7721 cells. BMC Cancer 2013; 13: 448.

[8] Mitsudomi T, Kosaka T and Yatabe Y. Biological and clinical implications of EGFR mutations in lung cancer. Int J Clin Oncol 2006; 11: 190-198.

[9] Park HJ, Min TR, Chi GY, Choi YH and Park SH. Induction of apoptosis by morusin in human non-small cell lung cancer cells by suppression of EGFR/STAT3 activation. Biochem Biophys Res Commun 2018; 505: 194-200.

[10] Atal S, Asokan P and Jhaj R. Recent advances in targeted small-molecule inhibitor therapy for non-small-cell lung cancer-an update. J Clin Pharm Ther 2020; 45: 580-584.

[11] Das D, Xie L, Wang J, Shi J and Hong J. In vivo efficacy studies of novel quinazoline derivatives as irreversible dual EGFR/HER2 inhibitors, in lung cancer xenografts (NCI-H1975) mice models. Bioorg Chem 2020; 99: 103790.

[12] Cadranel J, Ruppert AM, Beau-Faller M and Wislez M. Therapeutic strategy for advanced

EGFR mutant non-small-cell lung carcinoma. Crit Rev Oncol Hematol 2013; 88: 477-493.
[13] Zhu P, Davis M, Blackwelder AJ, Bachman N, Liu B, Edgerton S, Williams LL, Thor AD and Yang X. Metformin selectively targets tumor-initiating cells in ErbB2-overexpressing breast cancer models. Cancer Prev Res (Phila) 2014; 7: 199-210.
[14] Peng M, Huang Y, Tao T, Peng CY, Su Q, Xu W, Darko KO, Tao X and Yang X. Metformin and gefitinib cooperate to inhibit bladder cancer growth via both AMPK and EGFR pathways joining at Akt and Erk. Sci Rep 2016; 6: 28611.
[15] Menendez JA, Quirantes-Piné R, Rodríguez-Gallego E, Cufí S and Joven J. Oncobiguanides: Paracelsus' law and nonconventional routes for administering diabetobiguanides for cancer treatment. Oncotarget 2014; 5: 2344-2348.
[16] Xiao D, Lu Z, Wang Z, Zhou S, Cao M, Deng J, Hu X, Peng M, He C, Wu J, Xu S, Zhang H, Xu C, Wang W, Guan A and Yang X. Synthesis, biological evaluation and anti-proliferative mechanism of fluorine-containing proguanil derivatives. Bioorg Med Chem 2020; 28: 115258.
[17] Gu XY, Jiang Y, Li MQ, Han P and Cui BB. Overexpression of EGFR regulated by RARA contributes to 5-FU resistance in colon cancer. Aging (Albany NY) 2020; 12: 156-177.
[18] Ullrich A and Schlessinger J. Signal transduction by receptors with tyrosine kinase activity. Cell 1990; 61: 203-212.
[19] Purba ER, Saita EI and Maruyama IN. Activation of the EGF receptor by ligand binding and oncogenic mutations: the "rotation model". Cells 2017; 6: 13.
[20] Howe LR and Brown PH. Targeting the HER/EGFR/ErbB family to prevent breast cancer. Cancer Prev Res (Phila) 2011; 4: 1149-1157.
[21] Wu Z, Zhu Q, Yin Y, Kang D, Cao R, Tian Q, Zhang Y, Lu S and Liu P. Traditional Chinese medicine CFF-1 induced cell growth inhibition, autophagy, and apoptosis via inhibiting EGFR-related pathways in prostate cancer. Cancer Med 2018; 7: 1546-1559.
[22] Li L, Fan P, Chou H, Li J, Wang K and Li H. Herbacetin suppressed MMP9 mediated angiogenesis of malignant melanoma through blocking EGFR-ERK/AKT signaling pathway. Biochimie 2019; 162: 198-207.

Table S1. The targeting oligos of EGFR

Sh EGFR-1	CGCAAAGTGTGTAACGGAATA
Sh EGFR-2	CATCAGTGGCGATCTCCACAT
Sh EGFR-3	CTGGATCCACAGGAACTGGAT

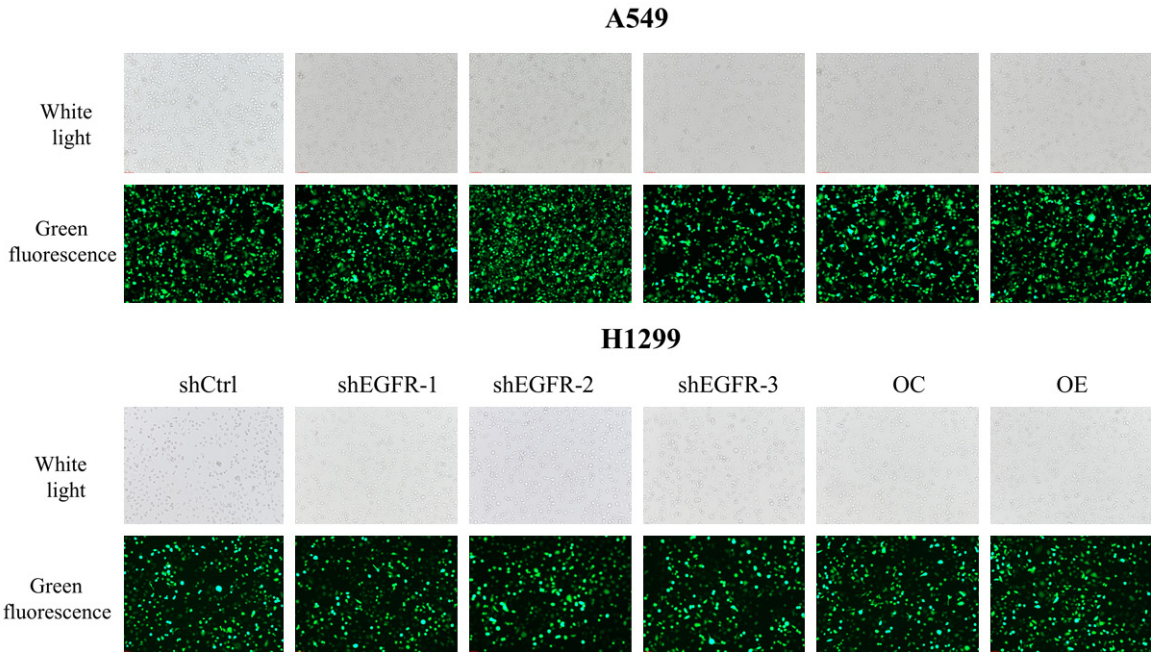

Figure S1. The ccreening of the A549 and H1299 cells with stable overexpression and EGFR knockdown. The cells were transfected with Sh Ctrl, Sh EGFR-1, Sh EGFR-2, Sh EGFR-3, OC, and OE lentiviral vectors for 12 h and then cultured in complete medium. Three days later, puromycin was added to the cell culture flask to kill the untransfected cells, and the screening efficiency was observed under a DFC450C microscope (Leica).